Assessment of the effect of defects on mechanical properties of adhesive bonded joints by using non destructive methods

DOI: https://doi.org/10.1016/j.compositesb.2016.01.059

Assessment of the effect of defects on mechanical properties of adhesive bonded joints by using non destructive methods

[2]Rosanna Tamborrino, [1]Davide Palumbo, [1]Umberto Galietti, [2]Patrizia Aversa, [2]Samanta Chiozzi, [2]Vincenza Anna Maria Luprano

[1]*Department of Mechanics, Mathematics and Management (DMMM), Politecnico di Bari, Viale Japigia 182, 70126, Bari (Italy),*

[2]*Enea Research Centre Brindisi, SS 7 "Appia" km 714, 72100 Brindisi (Italy).*

Corresponding author: Davide Palumbo, email: davide.palumbo@poliba.it, phone: 3495990841

Abstract

Mechanical performance of the adhesive joints depends on many parameters including width, depth and continuity of the adhesive layer applied. In this work, lock-in thermography and ultrasound methods were used to detect the dimension of defects of adhesive joints while tensile tests were carried out to assess their strength and stiffness. Both the effect of bond defects and the possibility to use non destructive method for the prediction of strength and stiffness of joints have been discussed considering a statistical analysis of data. Models, useful for predicting mechanical behaviour of joints on the basis of their defects, have been developed.

Key words: lock-in thermography, ultrasonics, defects, mechanical properties, glass fibres.

1.Introduction

Advanced composite materials are widely used in high technology structures because of their high performance in terms of high moduli, high corrosion, fatigue and tensile resistance, and low weight [1]. But almost every designed structure requires component members to be connected. Adhesive bonding is a joining method with high potential which has been reviewed in detail [2]. With new composite materials being introduced in the market, adhesives become the number one choice to joint composite structures [3], [4]. An adhesive joint is an optimal type of joining composite materials as it allows a uniform load distributing over a larger area than other methods of joining, requires no holes, adds very little weight to the structure and has superior mechanical resistance. Mechanical performance of the adhesive joints depends on many parameters including width, depth and continuity of the adhesive layer applied [5].

Although adhesively bonded joints have many advantages over other structural joining methods, mainly related to their efficient load transfer in thin components and structural repairs, their general application has suffered due to the difficulty in inspecting bondline quality following manufacture and in-service life [6] and sensitivity of bondline integrity to environmental attack and physico-chemical conditions of the substrates. In this regard, different works in literature deal with the adhesive joint behavior under static loading and dynamic ones by means of numerical and experimental approaches [7], [8]. In particular, in his work Ascione [9] showed the numerical results about the influence of an adhesion defect on the ultimate capacity of an adhesive double lap joint.

Complete voids, disbonds and porosity are the simplest forms of defect to detect non-destructively and the majority of non-destructive testing performed on bonded structures aims to detect such defects [10].

Hart-Smith [11], discussed the effects of any flaws and porosity on the shear load transfer for both thin and thick adherends. A significant effect of bond defects is obtained in the case that the dimension of defect is large enough to alter the distribution of the load transfer through the bond and if it is located at the ends of the overlap. Thus, the importance of non-destructive

characterization (NDE) of composites and their structures grows with the increasing use of these materials and it is necessary to ensure industry requirements for safety and reliability of materials and their structures.

During the production phase, and also in service with critical structures, it is essential to use non-destructive tests to assess the quality and fitness for the purpose of the product. The non-destructive test does not measure strength directly but measures a parameter which can be correlated to strength. It is, therefore, essential that a suitable non-destructive test is chosen and that its results are correctly interpreted. The objective of any form of non-destructive test is to correlate the joint strength with some physical, chemical or other parameter that can be measured without causing damage.

Acoustic imaging methods and thermography are some of the diffused choices among non-destructive techniques as they allow not only to detect the presence of defects but also to characterize them in terms of size, shape, and location [5], [12], [13-18].

In this paper, the effect of bond defects on mechanical properties of adhesive bonded joints were evaluated in terms of strength and stiffness. In particular, both destructive and non destructive tests were carried out on adhesive joints designed according to ASTM D 3165. Lock-in thermography and ultrasound methods were used to assess the dimension of defects while tensile tests were carried out to assess their strength and stiffness. Both the effect of bond defects and the possibility to use non destructive method for the prediction of strength and stiffness of joints have discussed considering a statistical analysis of data.

2.Experimental materials and methods

2.1 Specimens

Single lap adhesive joints have been prepared according to ASTM D 3165 using glass fiber reinforced thermosetting plastic (vinyl ester GFRP) substrate and a two part epoxy adhesive:

AME6000 INF (Ashland Composite Polymers) and ADH 90.91 (Altana Electrical Insulation) [10]. Adherends are characterized by multiple layers of quadriaxial 0°/+45°/90°/-45° fabric glass fiber and have been obtained from a laminate produced with the technique of infusion of the resin under vacuum (VARI). Surface preparation has been carried out according to ASTM D 2093 for surface preparation of plastics [19]. The panels, properly cleaned and treated, have been placed inside a tool for bonding where they have been lined up by reference pins. After spreading a thin layer of adhesive, the assembly has been closed and the pressure has been applied. As regards the care conditions, they have been observed as indicated by the manufacturer of adhesive. To limit as much as possible any misalignment problems and effects connected with it, the application of tabs glued on adherends has been provided. This arrangement moves the average of load exactly in the centerline of the adhesive [20].

Since the regulation [20] refers to the use of metals, while the present study is based on adherends in composite materials, changes have been made, in the thickness of the adherends, which are set to a value of 2.5 mm, while the thickness of the adhesive remains equal to 0.76 mm. The planar and three-dimensional geometry of the joints are shown in Figure 1.

The single-lap samples have been cut from the panels according to the scheme shown in Figure 2. Specimens were cut using water-jet cutting to avoid machining defects and to maintain a good surface finish from the fabricated laminates. Moreover, a preliminary visual testing was carried out before performing the bonding.

A total amount of 21 samples have been used for the experimental tests and they have been denoted by the initials VA followed by a sequential cardinal number and the indication of the production lot.

2.2 Lock-in thermographic analysis

Lock-in thermography is based on the generation of thermal waves inside the specimen, for example, by depositing heat periodically on the specimen surface [13], [14]. The resulting oscillating temperature field in the stationary regime can be recorded remotely through its thermal

infrared emission by an IR camera. Thermal wave can be reconstructed by measuring temperature evolution over the specimen surface: by a suited algorithm, information about magnitude (A) and phase (φ) of the thermal wave can be obtained.

Phase data are relatively independent of local optical and infrared surface features and phase signal allows to penetrate deeper into the material than the analysis of the magnitude signal.

In the phase image, the defects appear with a different phase signal respect to the homogeneous material. Moreover, the phase of thermal wave is related directly to depth z [14].

Lock-in thermography tests were performed by IR camera FLIR SC640 with thermal sensitivity (NETD) < 30 mK and based on a microbolometer detector with 640×512 pixels.

The set-up used is shown in Figure 3 ($\beta = 30°$, $D_T = 30$ *cm*, $D_L = 20$ *cm*). In particular two halogen lamps with power 500 W were controlled by MultiDES® system in order to heating specimens with a series of sinusoidal waves. For each single lap joint sample, the area over the bonding, showed in figure 4 was investigated. Thermal data were processed by IRTA® software in order to obtain amplitude and phase images [12].

2.3 Ultrasonic analysis

The ultrasonic C-scan technique is considered well established in literature for the debonding detection of joints [21], [22], therefore ultrasonic tests were also carried out in order to assess the correctness of the results obtained using lock-in thermography [12], [23].

All single-lap joint sample were subjected to a volumetric UT scanning analysis procedure. UT images for any portion of the material thickness can be obtained and analyzed.

The UT inspection technique chosen for this study was the "pulse - echo" and the coupling of ultrasound has been realized with driven jets of water. The probe for this application was a focused immersion transducer of 1 MHz frequency. Water and GFRP material UT speed were 1483m/s and 2578m/s, respectively. For each single lap joint sample, a 80 mm x 24 mm area over the bonding

was scanned with a 0.2 mm scan step. In figure 5 are shown the obtained UT images related to the first interface adhering/adhesive of the joints VA01 and VA03.

2.4 Mechanical tests

Tensile tests have been performed at room temperature, according to ASTM 3039 [20]. All the mechanical tests have been machined with the same geometry, according to ASTM D3165 (Figure 1). Tests have been executed with the electromechanical test machine MTS Alliance RT/50, with a load cell of 50 kN, and with a rate of 2 mm/min. A uniaxial extensometer with a gage length of 12.5 mm has been used to monitor the deformation of the joint in the overlap length.

In Fig. 6 there is an overall view of the setup of the test used and the detail of a joint under test.

3. Results and discussion

3.1 Non destructive test results

Lock-in tests were carried out considering only one side of specimen and then defect was detected at the first interface adhering/adhesive. Different preliminary tests were carried out on a reference sample specimen, called VA0, in order to assess the optimum value of the modulation frequency for lock-in thermography tests. The optimum modulation frequency (0,0125 Hz) was obtained by considering the procedure described in the work [12].

Figure 7 shows the phase images obtained by IRTA® software of all specimens. Black areas indicate the presence of bond defects while green lines delimitate the area of interest. Almost all specimens seem affected by debonding.

A quantitative thermographic and UT data analysis was carried out in order to identify the defects using a decision threshold values criterion. In this way, the detectable and undetectable defects are

expressed as 1 and 0 (hit/miss data), respectively and it is possible a comparison between techniques. The threshold value *Th* was defined through a statistical analysis of data [12],[25]. Phase images and ultrasonic images processed using the chosen threshold value criterion show almost the same equivalent normalized bonded area. Lock-in Thermographic results agree with the ultrasonic inspection, thus its capability to locate and identify defects into bonded joints is validated [12], [23]. In Figure 8, pictures of the broken specimens are reported in comparison with the non-destructive results shown in binarized phase and UT images.

3.2 Mechanical characterization

A Light-fiber-tear failure (LFT), has been observed for all joints. This kind of failure is described by Standard ASTM D 5573-99 and happens within the composite matrix near the surface [26]. Visual inspection of the broken specimens confirms the presence of defects as identified by non destructive tests, with correct shapes and size. They appear located at the ends of the overlap. Table 1 shows the tensile data for all joints, in terms of shear modulus (G) and shear stress (τ_{max}). The values of the debonded area measured on the thermography images are included for comparison in the second column. In the last columns of Table 1, the specimens are grouped in different classes in order to perform a statistical analysis that will be reported in the following section.

It can be observed that both the strength and stiffness of the joints is influenced by the percentage of debonded area. It is seen that the mechanical behavior is worsened decreasing the bonded area. The trend of the load in function of the displacement has been plotted for each test (Figure 9). In the tests, a considerable linearity of the load-displacement diagrams up to the maximum value, for all joints can be noticed. The results are presented in Fig. 8 in comparison with that of the joint VA07, which is completely bonded. In this way, it immediately appears as the strength and stiffness of the joints is influenced by the percentage of bonded area.

3.3 Statistical analysis

A statistical processing of data can be performed in order to verify if the presence of bonded defects is significant in terms of mechanical properties variations of joints.

Defected areas evaluated from thermographic images has been considered for performing this analysis. It is possible because of the previous validation of them with ultrasonic images. As just said in the previous section, by grouping the available results, first in 2 classes and then in 5 classes, as shown in Tab. 1, and applying the analysis of variance (ANOVA), the variations in G and τ_{max} due to the changes in debonded areas result significant. ANOVA is a statistical instrument, developed in order to verify the significance of the differences between the arithmetic means of two or more similar statistical populations [27].

In this work, the assessments have been performed by decomposing the totality of the data into groups where only one parameter changes at a time. A statistically significant result, when a probability (p-value) is less than a pre-determined threshold (significance level), justifies the rejection of the null hypothesis. In particular, after having verified the significance relatively to 2 macro classes ($A_{(50 - 76)\,\%}$ and $B_{(77- 100)\,\%}$), the division of data into 5 classes ($A_{(50\text{-}59)\,\%}$, $B_{(60\text{-}69)\,\%}$, $C_{(70\text{-}82)\,\%}$, $D_{(83\text{-}90)\,\%}$, $E_{(91\text{-}100)\,\%}$) has been performed to evaluate in detail the significance at a particular percentage of the debonded area on the variations of G and τ. The changes in G is influenced by the debonded area, stopping at the class *D*, that is the significance is not more appreciable. Whereas, *C* is the critical class for τmax.

The results of ANOVA tests, executed using the software MINITAB^{TM} , previously commented, are reported below (Table 2, 3, 4, 5 and Figure 10, 11).

An attempt to create possible mathematical models to describe the mechanical behavior of bonded joints depending on the percentage of debonded area has been performed.

The models have been obtained by considering the mechanical properties (G and τ_{max}), as a function of the percentage of debonded area. In this way, it is possible to see how the mechanical

characteristics of the joints decay as a function of the equivalent debonded area. The goodness-of-fit statistics of the 2 models are reported in Table 6 and 7.

In order to have a quicker idea of the decay of the characteristics, in figures 12 and 13 the values of the elastic modulus and *UTS* are presented normalized with respect to their maximum values. As it can be seen in these figures, a mean decay of about 55% on the shear modulus and about 20% of the shear strength can be observed within 0-48% range of debonded area.

The result of fitting is better for the shear modulus, while the model for the shear stress approximates worse the data, even if the significativity is acceptable. It is clear by observing the tables related to the goodness of fit statistics.

4. Conclusions

This work presents results from an experimental study on the efficiency of thermographic techniques validated by ultrasonic as nondestructive testing of adhesive GFRP joints.

The primary objective has been the investigation of the goodness of bonds at the interface between adherends of a composite joint and it has been followed by the evaluation of the possible relation between defects in the bonded interface of a joint and its mechanical properties.

The thermographic lock-in method provided the experimental basis to examine the joints on a quality level, while a quantitative understanding of their structural shear behavior was obtained through a mechanical characterization testing and a statistical analysis of data. The analysis of the statistical results shows that the strength and stiffness of the joints are influenced by the percentage of debonded area. Supported by statistical results, two models, useful for predicting mechanical behavior of joints on the basis of their defects, have been developed. The result of fitting is better for the shear modulus, but both shear modulus and shear stress decay with the increasing of equivalent lacked area. It implies that the mechanical behavior of the GFRP single lap joints is worse decreasing the bonded area.

Acknowledgments

The described study was performed throughout the course of the research and technological development project PS 095 “Innovative materials and methodologies for products in renewable energy sector (MIPER)” founded by the regional Apulia government.

References

[1] Baker S, Dutton S, Kelly D. Composite Materials for aircraft Structures. American Institute for Aeronautics and Astronautics, Ins., Reston, Virginia, 2004.

[2] Adams RD. Adhesive bonding: science, technology and applications. Woodhead Publishing, 2005.

[3] Higgins A. Adhesive bonding of aircraft structures. Int. J. Adhesion Adhesives 2000; 20(5): 367–376.

[4] Oterkus E, Barut A, Madenci E, Smeltzer III SS, Ambur DR. Bonded lap joints of composite laminates with tapered edges. Int. J. Solids Structures 2006; 43:1459–1489.

[5] Maeva EY, Severina I, Wehbe H, Erlewein J. Ultrasonic Imaging Techniques to Evaluate Quality of Fiber Reinforced Composite Materials and their Adhesive Joints. In: 5th Pan American Conference for NDT, Cancun, Mexico, 2-6 October 2011.

[6] Butkus LM, Johnson WS. Designing for the durability of bonded structures. Presented at the FAA/NASA symposium on continued airworthiness of aircraft structures, Atlanta, 1996. p. 28–30.

[7] Sawa T, Temma k, Tsunoda Y. Axisymmetric stress analysis of adhesive butt joints of dissimilar solid cylinders subjected to external tensile loads. International Journal of Adhesion and Adhesives, 1989;9(3):161-169.

[8] Sato C. Dynamic stress responses at the edges of adhesive layers in lap strap joints of half-infinite length subjected to impact loads. International Journal of Adhesion and Adhesives, 2009;29:670-677.

[9] Ascione F. The influence of adhesion defects on the collapse of FRP adhesive joints. Composites Part B, 2016;87: 291-298.

[10] Adams RD, Drinkwater BW. Nondestructive testing of adhesively-bonded joints. NDT&E International, 1997; 30 (2):93-98.

[11] Hart Smith LJ. Effect of flaws and porosity on strength of adhesive-bonded joints. In: 29th Annual Sampe Symposium and Technical Conference, Reno, Nevada, April 3-5, 1984.

[12] Palumbo D, Tamborrino R, Galietti U, Aversa P, Tatì A, Luprano VAM. Ultrasonic analysis and lock-in thermography for debonding evaluation of composite adhesive joints. NDT & E International, In Press, Accepted Manuscript, Available online 10 September 2015, doi:10.1016/j.ndteint.2015.09.001.

[13] Maldague X. Applications of infrared thermography in non-destructive evaluation. Universitè Laval, Quebec City (Quebec), G1K 7P4, Canada, 2000.

[14] Maldague X. Theory and practice of infrared technology for non-destructive testing. Wiley Series in microwave and optical engineering, Kai Chang, Series Editor, 2001.

[15] Tashan R, Al-mahaidi R. Investigation of the parameters that influence the accuracy of bond defect detection in CFRP bonded specimens using IR thermography. Composite Structures, 2012; 94:519-133.

[16] Genest M, Martinez M, Mrad N, Renaud G, Fahr A. Pulsed thermography for non-destructive evaluation and damage growth monitoring of bonded repairs. Composite Structures, 2009; 88:112-120.

[17] Schroeder JA, Ahmed T, Chaudhry B, Shepard S. Non-destructive testing of structural composites and adhesively bonded composite joints: pulsed thermography. Composites: Part A, 2002; 33:1511-1518.

[18] Galietti U, Dimitri R, Palumbo D, Rubino P. Thermal analysis and mechanical characterization of GFRP joints. In: 15th European Conference on Composite Materials: Composites at Venice, ECCM 2012, Venice, Italy, 24-28 June, 2012.

[19] ASTM D2093 – 03: Standard Practice for Preparation of Surfaces of Plastics Prior to Adhesive Bonding, 2013.

[20] ASTM D3165 – 07: Standard Test Method for Strength Properties of Adhesives in Shear by Tension Loading of Single-Lap-Joint Laminated Assemblies, 2014.

[21] Segal E, Rose JL. Non-destructive testing of adhesive bond joints. Research Techniques in Nondestructive Testing, 1980; 4:275-315.

[22] Adams RD, Cawley P. Defects types and non-destructive testing techniques for composites and bonded joints. Construction and Building Materials, 1989; 3:170-183.

[23] Tamborrino R, Aversa P, Tatì A, Luprano VAM, Galietti U, Palumbo D. Ultrasonic and Thermographic Analysis of Composite Adhesive Joints Subjected to Accelerated Aging. In: 11th European Conference on Non-Destructive Testing (ECNDT 2014), Prague 2010, Oct 6-11, 2014.

[24] ASTM D3039: Standard Test Method for Tensile Properties of Polymer Matrix Composite Materials, 2014.

[25] Palumbo D, Ancona D, Galietti U. Quantitative damage evaluation of composite materials with microwave thermographic technique: feasibility and new data analysis. Meccanica, 2015; 50:443-459.

[26] ASTM D 5573-99: Standard practice for classifying failure modes in fiber-reinforced-plastic (frp) joints, 2005.

[27] Montgomery DC, Runger GC. Applied Statistics and Probability for Engineers. John Wiley & Sons, Inc, 2003.

Figures

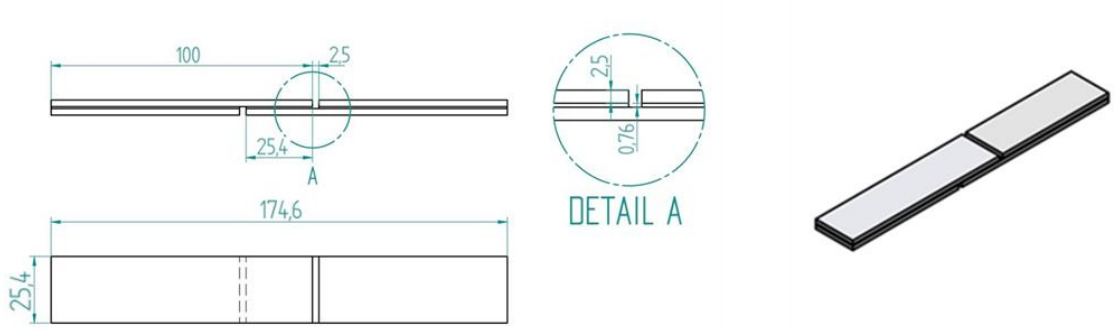

Figure 1: Planar and three-dimensional geometry of the joints

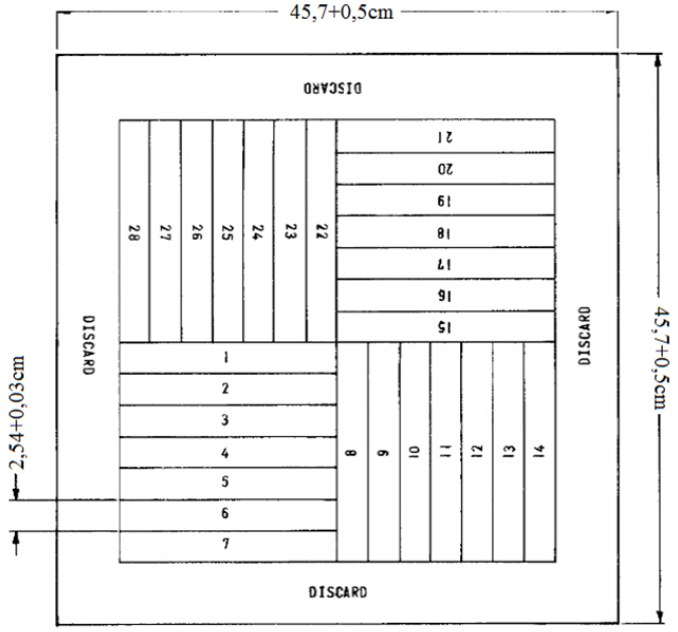

Figure 2: Geometry of the panel according to ASTM D 3165

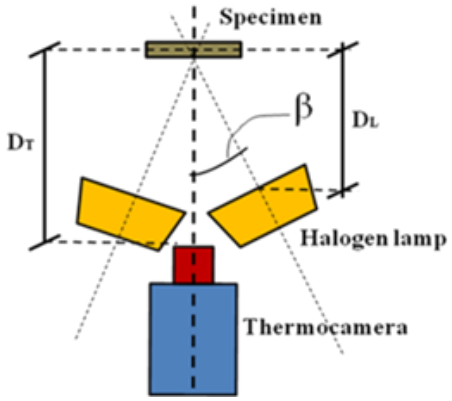

Figure 3. Schematic set-up used for lock-in thermography ($\beta = 30°$, $DT = 30\ cm$, $DL = 20\ cm$)

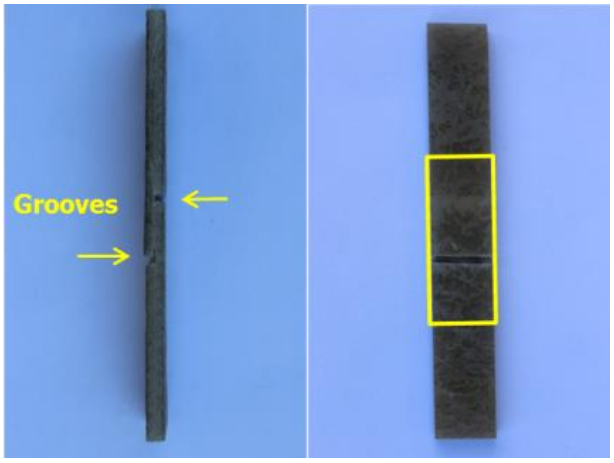

Figure 4. Investigated area by non-destructive methods

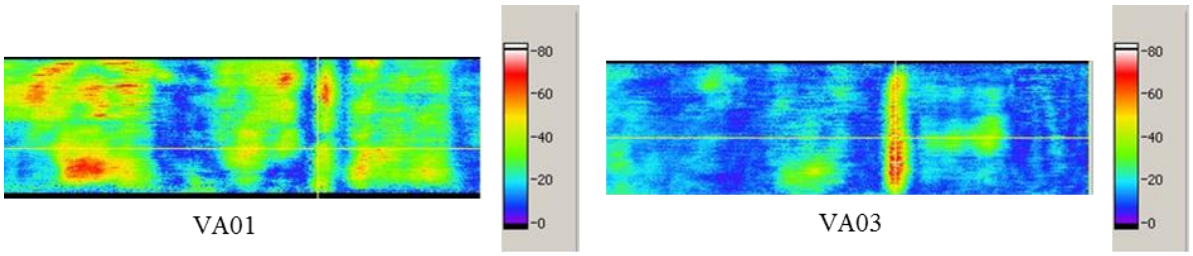

Figure 5. UT images single-lap joints VA01 and VA03

Figure 6. Setup of tensile test and detail of a joint under test

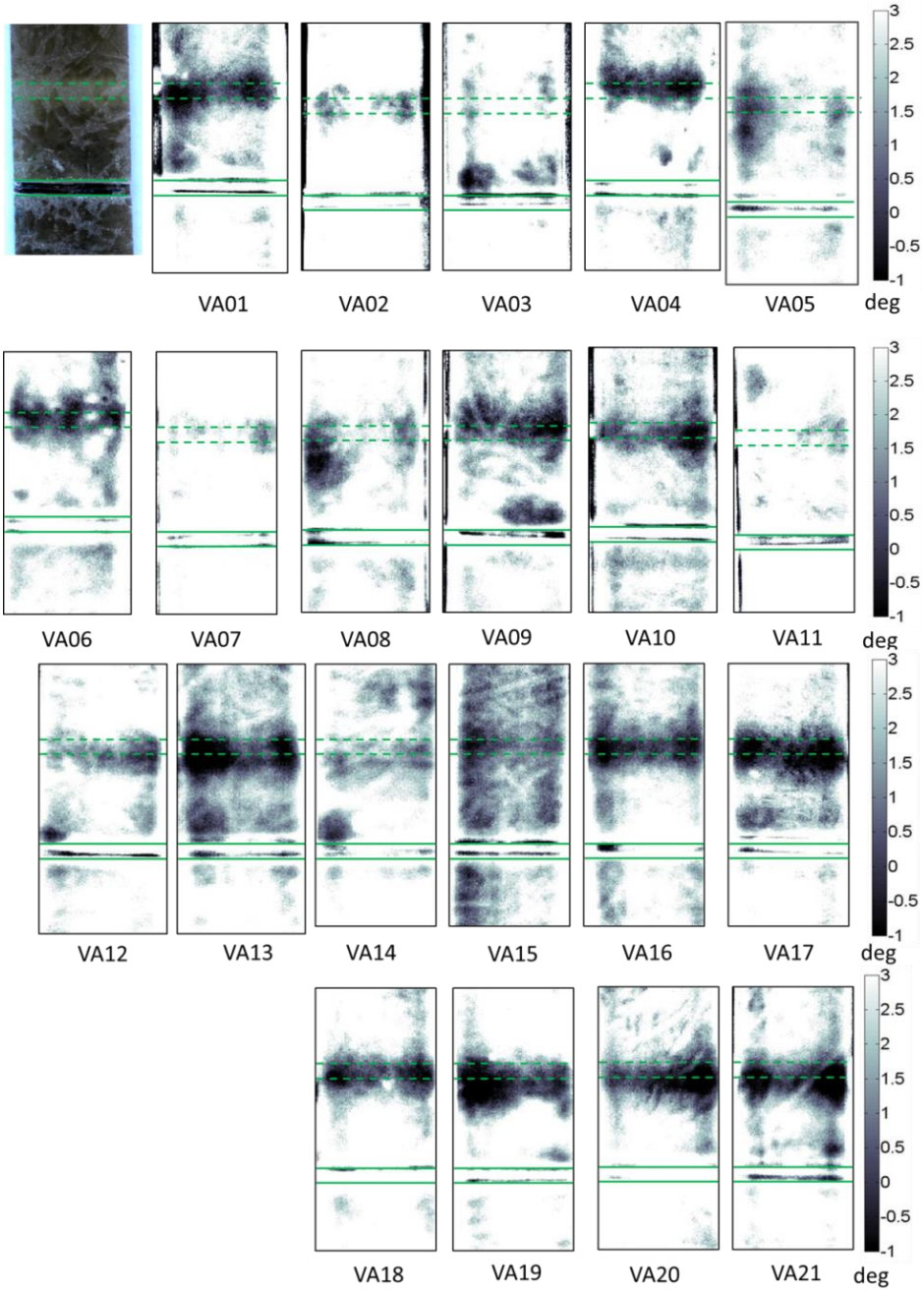

Figure 7. Phase images obtained with a modulation frequency of 0,0125 Hz.

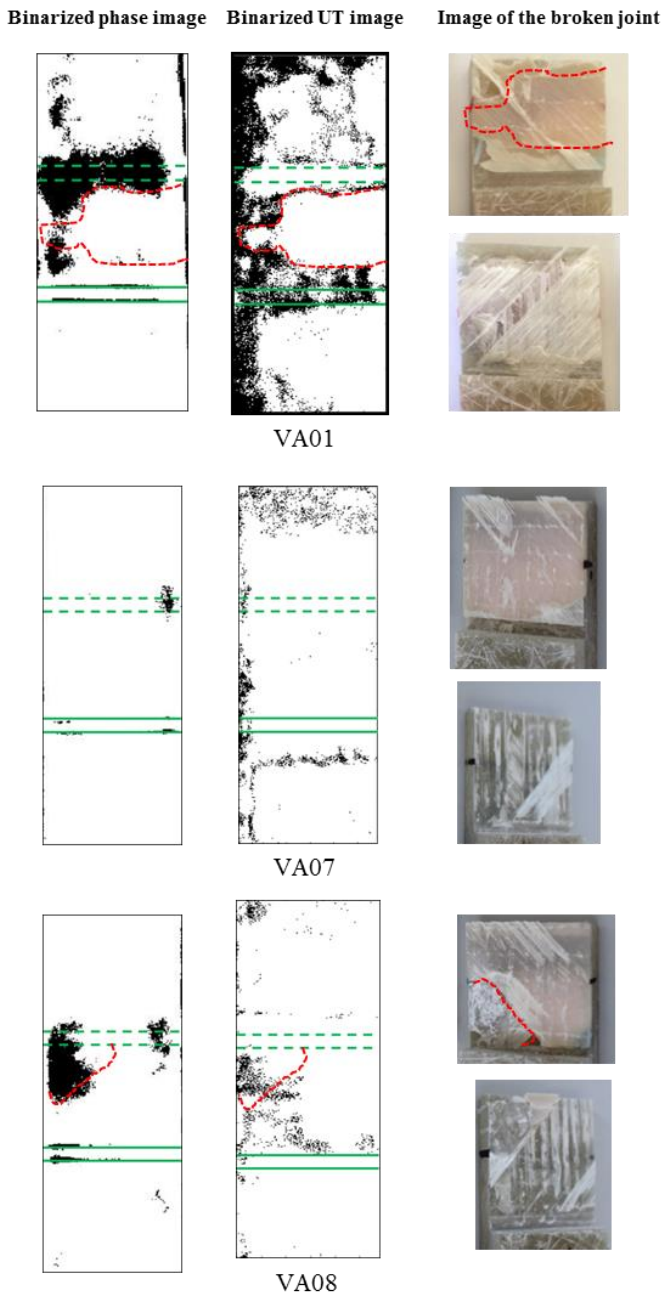

Figure.8. Binarized phase images, binarized UT images and images of the broken joints of the samples VA01, VA07, VA08 [9]

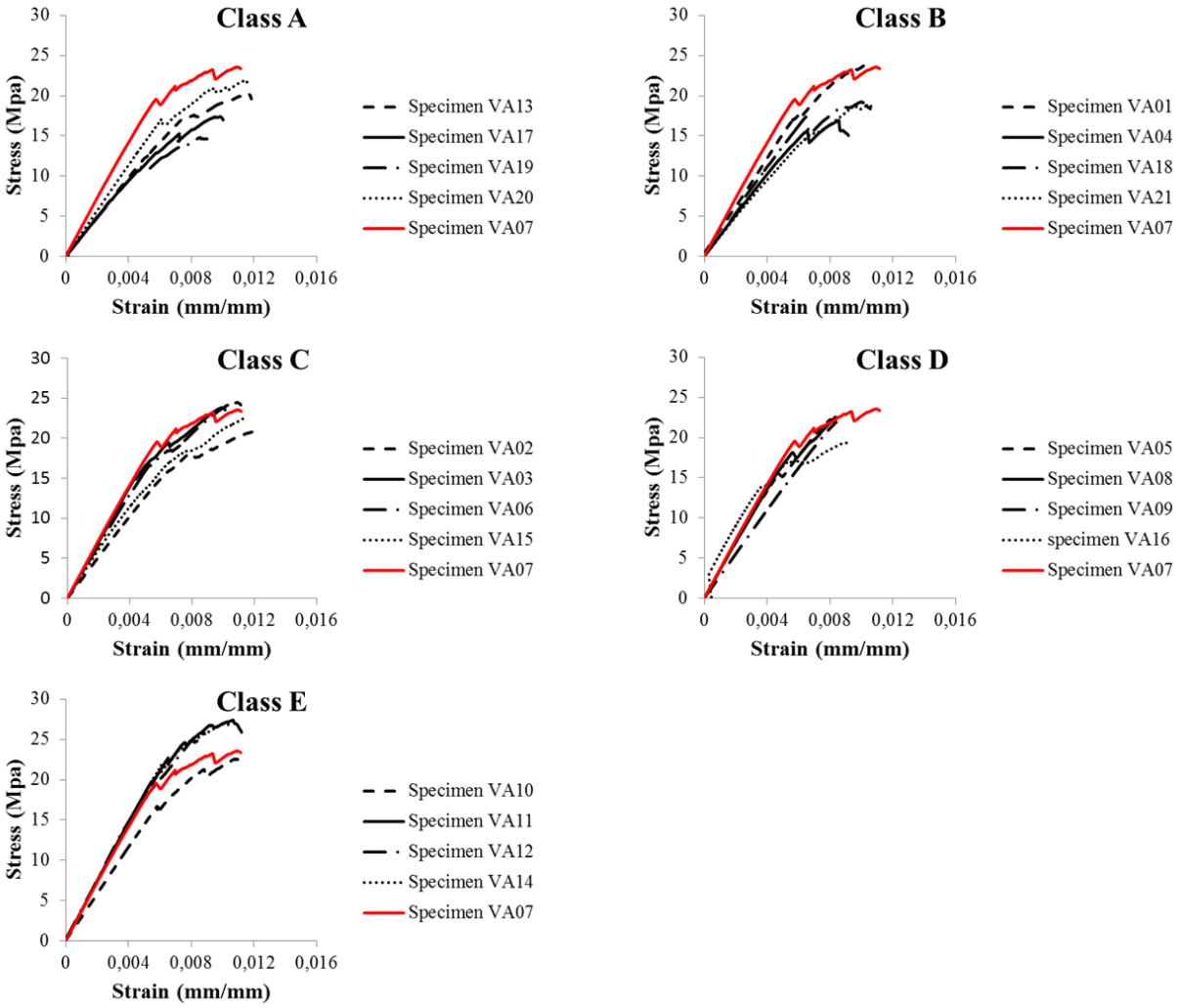

Figure 9. Stress-Strain diagrams of all joints compared with Stress-strain diagram of the joint VA07

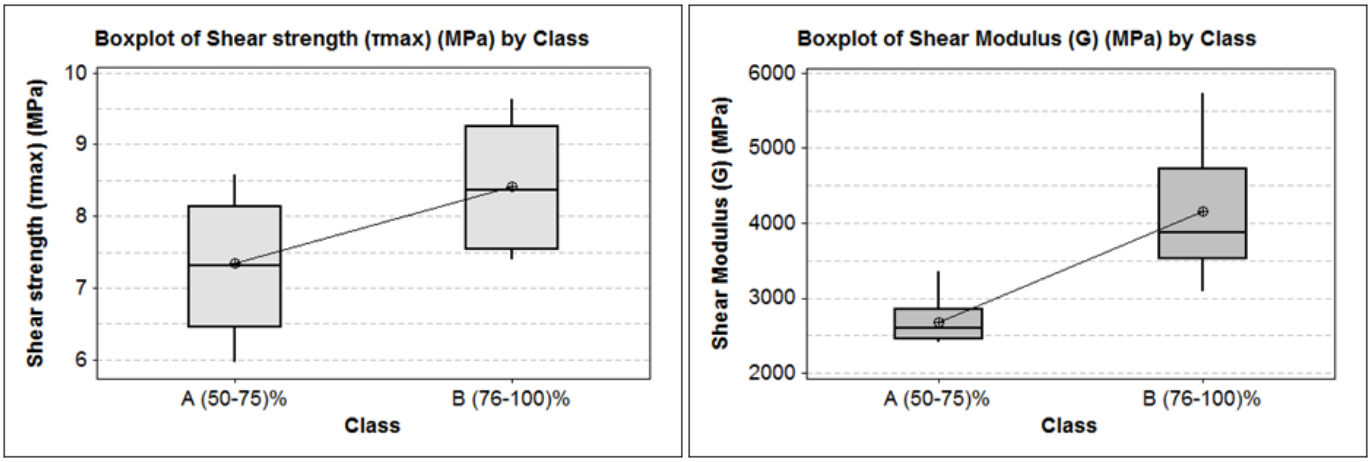

a) b)

Figure 10. a)Boxplot of shear modulus by class choosing 2 classes and b) Boxplot of shear strength by class choosing 2 classes

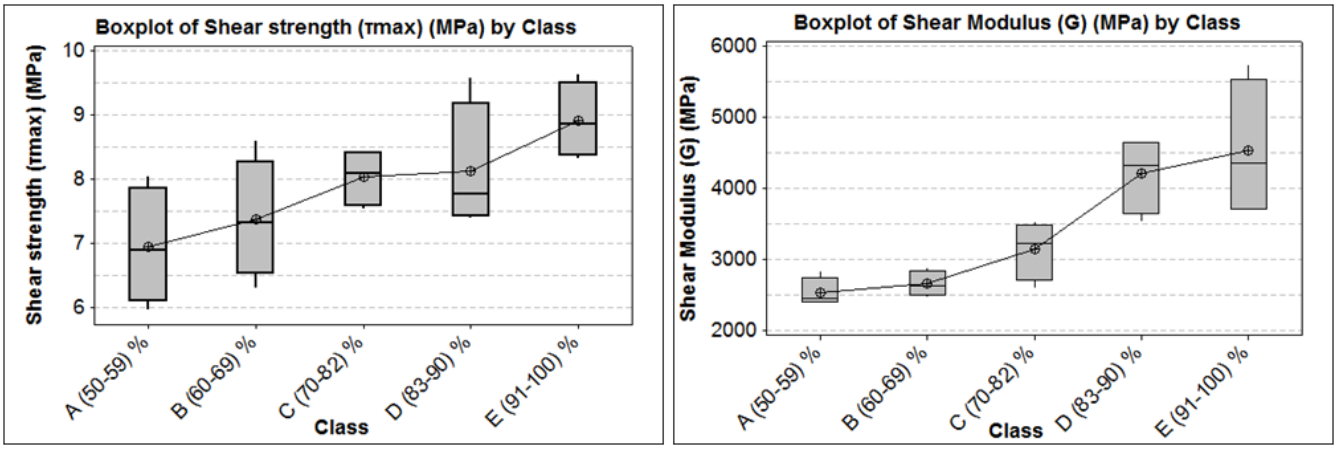

a) b)

Figure 11. a) Boxplot of shear modulus by class choosing 5 classes and b) Boxplot of shear strength by class choosing 5 classes

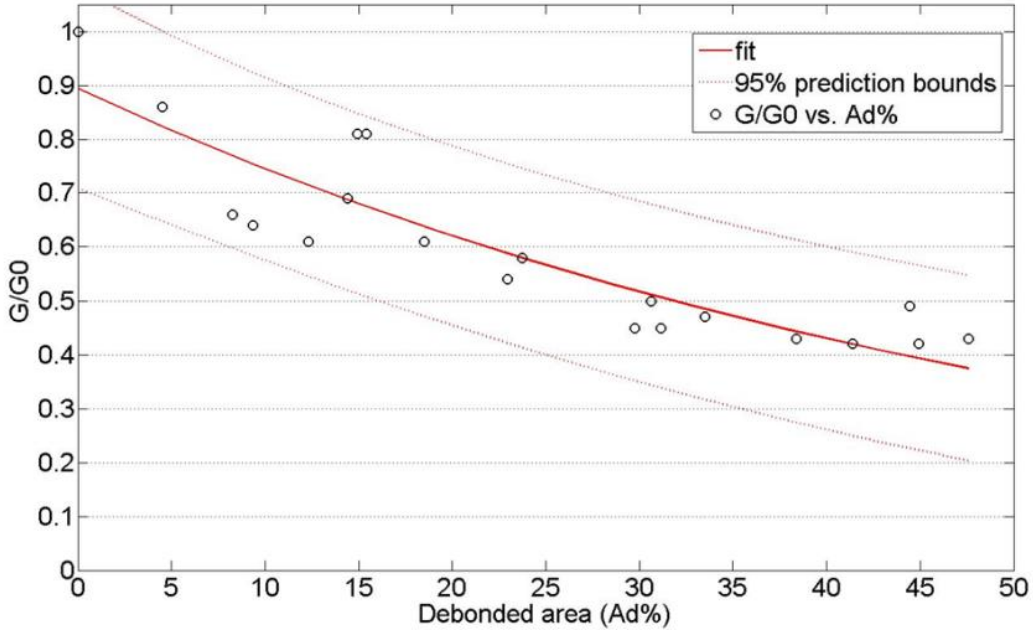

Figure 12. Curve Fitting for shear modulus

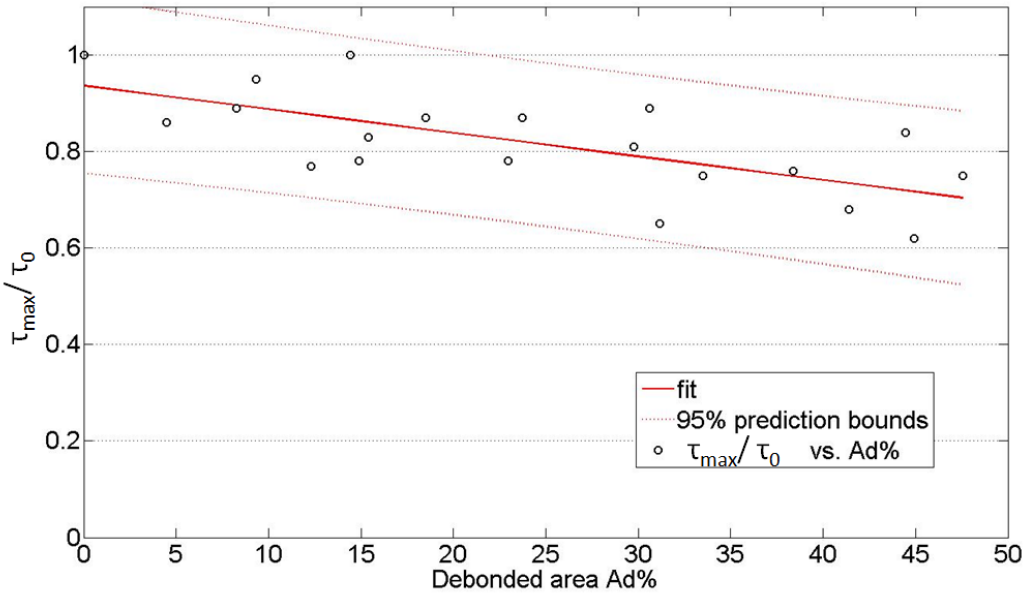

Figure 13. Curve Fitting for shear strength

Tables

Table 1: Tensile and non destructive data

Specimens	**Debonded area (%)**	**Shear modulus G (MPa)**	**Shear strength τ_{max} (MPa)**	**Classes**	
VA13	47,56	2461,60	7,26	A (50 - 76) %	A (50-59) %
VA19	44,92	2401,70	5,96		
VA20	44,44	2838,50	8,04		
VA17	41,41	2427,80	6,51		
VA21	38,38	2471,60	7,35		B (60-69) %
VA18	33,50	2672,40	7,27		
VA04	31,14	2583,20	6,29		
VA01	30,62	2890,60	8,58		
VA02	29,77	2594,10	7,78		C (70-82) %
VA06	23,74	3356,30	8,38		
VA15	22,94	3079,20	7,53	B (77- 100)%	
VA03	18,49	3524,20	8,42		
VA09	15,40	4654,36	7,97		D (83-90) %
VA08	14,91	4646,15	7,54		
VA16	14,42	3987,40	9,58		
VA05	12,31	3528,00	7,39		
VA14	9,34	3690,80	9,13		E (91-100) %
VA12	8,27	3772,00	8,59		
VA10	4,50	4935,04	8,31		
VA11	0,02	5739,08	9,63		
VA07	0,00	5025,10	8,42	(100) %	

Table 2: ANOVA result related to shear modulus for data subdivided into 2 classes

Source	**DF**	**SS**	**MS**	**F**	**P**
Class	1	11038647	11038647	29,56	0,000
Error	18	6721804	373434		
Total	19	17760451			
S = 611,1		R-Sq = 62,15%		R-Sq(adj) = 60,05%	
Level	**N**	**Mean**	**St Dev**		
A(50-75)%	10	2669,8	293,4		
B(76-100)%	10	4155,6	812,9		

Table 3: ANOVA result related to shear strength for data subdivided into 2 classes

Source	**DF**	**SS**	**MS**	**F**	**P**
Class	1	5,692	5,692	7,77	0,012
Error	18	13,193	0,733		
Total	19	18,886			
S = 0,8561		R-Sq = 30,14%		R-Sq(adj) = 26,26%	
Level	**N**	**Mean**	**St Dev**		
A(50-75)%	10	2669,8	293,4		
B(76-100)%	10	4155,6	812,9		

Table 4: ANOVA result related to shear modulus for data subdivided into 5 classes

Source	**DF**	**SS**	**MS**	**F**	**P**
Class	4	13236135	3309034	10,97	0,000
Error	15	4524316	301621		
Total	19	17760451			
S = 549,2		R-Sq = 74,53%		R-Sq(adj) = 67,73%	
Level	**N**	**Mean**	**St Dev**		
A(50-75)%	4	2532,4	205,5		
B(76-100)%	4	2654,5	177,6		
C (70-82) %	4	3138,5	406,6		
D (83-90) %,	4	4204,0	548,4		
E(91-100) %	4	4534,2	984,0		

Table 5: ANOVA result related to shear stress for data subdivided into 5 classes

Source	**DF**	**SS**	**MS**	**F**	**P**
Class	4	9,148	2,287	3,52	0,032
Error	15	9,738	0,649		
Total	19	18,886			
S = 0,8057		R-Sq = 48,44%		R-Sq(adj) = 34,69%	
Level	**N**	**Mean**	**St Dev**		
A(50-75)%	4	6,9425	0,9051		
B(76-100)%	4	7,3725	0,9382		
C (70-82) %	4	8,0275	0,4424		
D (83-90) %,	4	8,1200	1,0039		
E(91-100) %	4	8,9150	0,5857		

Table 6: Mathematical model for shear modulus and its goodness-of-fit statistics

General model Exp1	f(x) = a*exp(b*x)
Coefficients (with 95% confidence bounds)	a = 0.8946 (0.8049, 0.9844) b = -0.01829 (-0.02291, -0.01367)
Goodness of fit:	SSE: 0.1071 R-square: 0.8014 Adjusted R-square: 0.7904 RMSE: 0.07712

Table 7: Mathematical model for shear stress and its goodness-of-fit statistics

Linear model Poly1	f(x) = p1*x + p2
Coefficients (with 95% confidence bounds)	p1 = -0.004884 (-0.007507, -0.00226) p2 = 0.9362 (0.8625, 1.01)
Goodness of fit:	SSE: 0.1115 R-square: 0.4594 Adjusted R-square: 0.4294 RMSE: 0.07869